SIMULATION OF SCATTERED EM FIELDS FROM ROTATING CYLINDER USING PASSING CENTER SWING BACK GRIDS TECHNIQUE IN TWO DIMENSIONS

M. Ho

Department of Electronic Engineering
WuFeng Institute of Technology
Taiwan

Abstract—In this paper, a new numerical technique, passing center swing back grids (PCSBG's) for the resolution of the grid distortion difficulty due to the rotational motion of objects is introduced. This proposed swing-back-grids approach alongside of the method of characteristics (MOC) is developed to solve EM scattering problems featured with rotating objects. The feasibility of such combination is apparent from the fact that MOC defines all field quantities in the centroid of the grid cell. The scattered EM fields from a rotating circular cylinder under the excitation of an EM pulse are predicted in two dimensions and the electric field distributions recorded at several time instances are demonstrated. In order to confirm that the cylinder is rotating and scattering EM fields simultaneously, the circular cylinder is uniformly divided into an even number of slices with one perfect reflector and one non-reflector alternatively since a rotating circular cylinder causes no relativistic effects.

1. INTRODUCTION

The EM scattering problems involved with moving objects have received a great deal of interest in the electromagnetic society since early 1970s. There have been many studies investigating this issue. Some studies focus on the derivation of the theoretical solutions for the EM scattering by perfect conductors in uniform translational motion [1–11], some on the EM scattering by linearly vibrating objects [12–14], some on the simulation of the scattered EM fields from perfect planes moving and vibrating [15–17], and one on a moving

---

Corresponding author: M. Ho (homt@mail.wfc.edu.tw).

dielectric half-space [18]. Among them, Harfoush et al. provided computational results, in addition to the theoretical analysis, by using the finite-difference time-domain (FDTD) technique, in which both Faraday's and Ampere's laws were employed as aides to respectively approximate the magnetic and electric fields immediately next to the moving surface whenever the surface travels away from the grid point [3]. The numerical simulations of the reflected EM fields from uniformly travelling and oscillating perfect plane were carried out using MOC in collaboration with the relativistic EM field boundary conditions, and the computational results revealed that the reflected fields disclose not only the modulations in phase and amplitude but also the Doppler shift in spectrum. It is also explained that, due to the movement of the boundary, some moments grid cells were gradually eliminated from the grid system, and for other certain moments, grid cells were introduced little by little into the grid system [15–18].

During the same decade, the analytical studies of EM scattering by rotating bodies were published by Van Bladel [19, 20]. However, numerically simulating the EM problems with rotating objects has been a dilemma when grid cells suffer from unrecoverable distortion. It is then the objective of this paper to introduce a new technique for the resolution of the grid distortion problem, to apply this proposed technique together with MOC for the solutions of EM scattering by rotating objects, and to provide numerical evidence of its practicability. This proposal is stemmed from the fact that all field components are defined in the center of the grid cell by MOC. In the MOC numerical procedure, it takes every metric term or change in geometry of each grid cell into account to evaluate the differential change in all field quantities within each grid cell for each time step. When working on an EM related problem with a dynamic boundary or rotating object, providing that all geometric changes of each distorted grid cell are accurately updated and that the sell distortion dilemma can be cured, one can compute the field magnitudes based on the existing MOC code with minor modifications tracing all changes in the deformed grid cells.

Nonetheless, the analytical study or numerical simulation the EM scattering by a rotating body is always intricate not to mention problems that lack symmetry of revolution or have complex configurations. Since return signal from rotating objects, such as helicopter's blades, may reveal useful information of the target under investigation, additional information may be of importance for communication systems on board and/or on ground [21–23]. Therefore resolving the grid distortion problem is a priority before one tries to solve the scattering problems by rotating objects.

2. PCSBG/MOC

The proposal of the use of PCSBG for the resolution of the cell distortion due to the rotating objects of interest is based on the fact that all field components are positioned in the center of grid cell by MOC. The feasibility of such an application is apparent because every field quantity is calculable if all details of the cell geometry can be precisely updated during the process, and the distorted grid cell can be recovered from deformation. The reasons are that MOC takes into account all metric terms of each cell to evaluate all fluxes across each cell face and that the swing-back-grids technique is devised to recover the deformed cells.

Prior to the introduction of the PCSBG technique, the grid system used in the present simulation is a modified version of the body-conforming O-type grid because the cylinder has a circular cross-section as depicted in Figure 1. From the diagram the followings are obvious. The cylinder is solid and placed at the center indicated by the thick solid line. The rest is air and composed of three zones of concentric grid cells. The most inner layer of cells designated as gap (between two solid lines) is an analogy to an electric motor, within which the so called swing-back-grids are defined. Finally, the grid number is doubled from one zone to the next because there must be an adequate number of grids for the shortest wavelength component of interest to ensure the numerical accuracy. This must be followed when one deals with EM related problems.
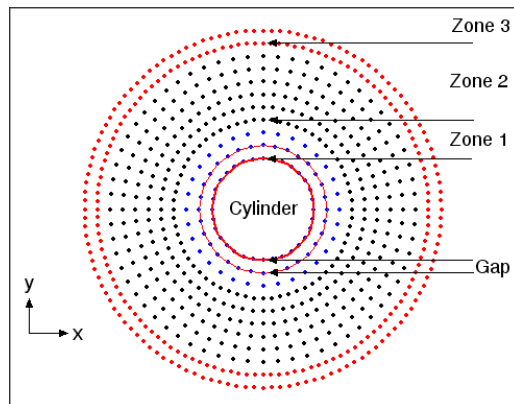

Figure 1. Representation of the modified O-grid in the Cartesian system. Grid number is doubled from zone to zone outward. One single layer of cells in the gap region is defined as PCSBGs.
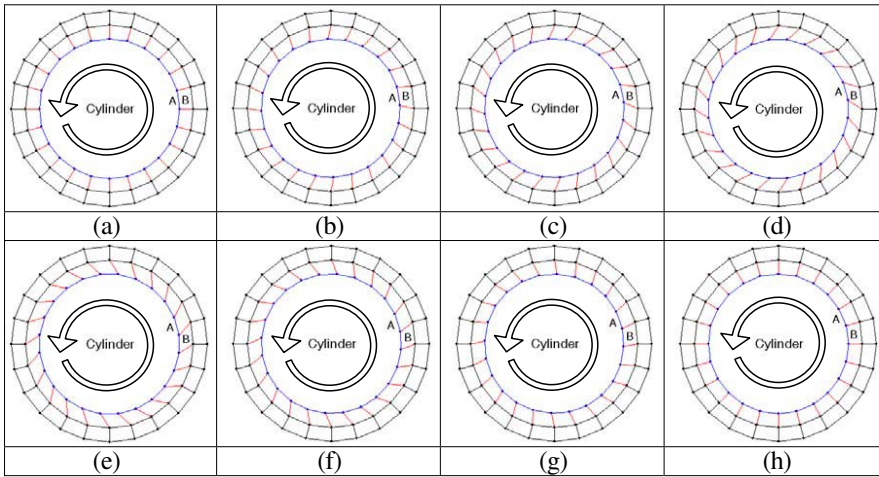
Figure 2. Sequential diagrams show how passing center swing back grids (PCSBG) work: (a) initial position, (b) cells are distorted, (c) distorted further, (d) grid points are about to pass the centroid, (e) grid lines had swung back, and (f)–(h) rotation goes on.

Given in Figure 2 are eight diagrams in sequential order illustrating how PCSBG operates. A quite coarse O-grid is used for clear demonstration, which includes a solid cylinder and only two layers of cells. Note that the grid cells are in trapezoidal shape and that the cylinder rotates counter-clockwise as pointed out. The outer layer of cells is fixed while the inner layer will be twisted since one side of the swing-back-grids is attached to and then moves along with the rotating cylinder. Also shown are the two letters A and B representing two different grid indices on the cylinder and in the gap, respectively. Figure 2(a) illustrates that the cylinder is about to rotate from a position where grid lines are aligned. In Figures 2(b) through 2(d), the swing-back-grids are skewed due to the rotation of cylinder as time advances. Note that the normal vector of the cell face on the cylinder surface is changing as cylinder rotates and that all grid lines are tilted. When each grid point on the cylinder side is about to pass the centroid of the grid cell and before cells distorted further as shown in Figure 2(d), all grid lines swing back as in Figure 2(e). At this point of time, all swing-back-grids are still skewed yet in the other direction. And the rotating cylinder now seems to straighten the distorted cells. Figures 2(f) through 2(h) exhibit that the cylinder continues rotating; especially in Figure 2(h), grid lines seem to resume the alignment positions yet with one index off. It is noticed that the

area of each swing-back-grid stays constant during the process, and consequently there is no need to adjust the numerical time step for these grids when they are skewed and even when their grid lines swing back.

3. THE PROBLEM

Consider the scattering problem by a rotating infinite long cylinder under the illumination of a Gaussian EM pulse and make a compromise between the computing resources and numerical performance; the problem is arranged as follows. The modified O-type grid system has a radius of 110 cm with a circular cylinder of 10 cm in radius located at the center and consists of five zones of cells. There are 144 cells in each layer in zone one around the cylinder; the number is doubled from zone to zone outward and ends up with 2304 cells each layer for the most outer zone. All cells are in the shape of trapezoid having identical thickness (along the radial direction) of about 6.2 mm and the other two dimensions ranging from 2.8 to 5.7 mm along the circumferential direction. It turns out to be about 162,000 cells in total. The excitation source is a plane Gaussian EM pulse with its electric field being normalized to unity and polarized to the positive z-axis as in Figure 3. As a result of having the incidence to propagate in the positive x-axis direction, the magnetic field component must be polarized to the negative y-direction. With a pulse width of 0.2 ns, the incident pulse accordingly has the highest frequency content of about 3.8 GHz. Given that there are at least 10 grids for the shortest wavelength component
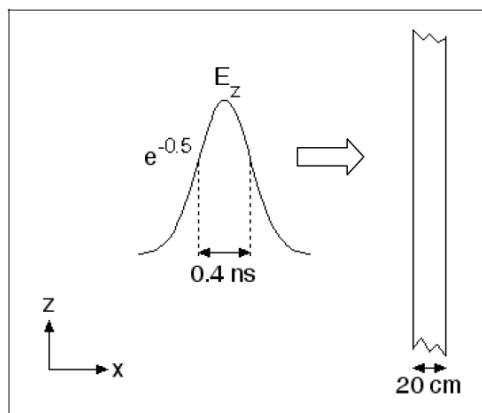

Figure 3. Schematic representation of the worked problem.

the minimum grid density is 128 points per meter. The minimum grid dimension is about 162 points per meter which meets the requirement. If the incident Gaussian pulse is truncated by a rectangular window with a cut-off level of 100 dB, it is then to have a span of about 1.92 ns end-to-end.

In order to have clear exhibition of the evidence that the cylinder is rotating and scattering EM fields simultaneously, further arrangement was made on the cylinder. The cylinder may be evenly sliced into an even number of sectors that are one perfect reflector and one non-reflector in turns as specified in Figure 4. Note that a solid radian line given in each case is to indicate the zero-angle position of the rotating cylinder before the counter-clockwise rotation is initiated and that around the cylinder thick arc lines represent perfect reflectors and thin ones represent the non-reflectors. For convenience, the number of turns made by the cylinder is defined on the basis of the Gaussian pulse span. Therefore, for a cylinder of 20 cm in diameter making a complete revolution within one Gaussian pulse span yields an angular velocity of about 1.09 times as fast as the light speed. This impractical arrangement along with the sliced cylinder is for the purpose of having clear pictures that cylinder is rotating and scattering EM fields at the same time.
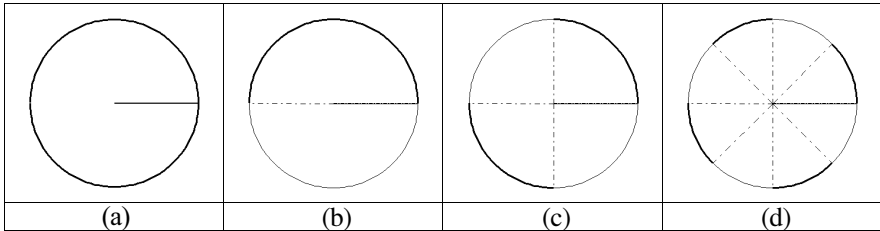

Figure 4. Sliced cylinders: (a) the whole cylinder, (b) two slices, (c) four slices, (d) eight slices. Thick arcs: Perfect reflector, thin arcs: Non-reflector.

Under such arrangement, there are three types of boundary conditions respectively used on the surfaces of reflectors and non-reflectors, and on most outer computational domain boundary. At the perfect reflector surface, MOC employs the characteristic variable (CV) boundary conditions which are inherent in MOC. The characteristic variables are defined as the product of the instantaneous variable vector and the eigenvector matrix. Therefore, each CV is associated with one particular eigenvalue and carrying information such as speed and direction which propagates across the cell surface. To evaluate the field

quantities on the perfect reflector surface, one has to make use of one particular CV that propagates onto the surface which is given by

$$\text{CV} = \hat{n} \times \vec{B} + \eta_o \vec{D} \tag{1}$$

where $\hat{n}$ is the normal vector of the grid on cylinder surface; $\vec{D}$ and $\vec{B}$ are the electric and magnetic flux density; and η_o is the characteristic impedance of free space. By definition, the CV in (1) is used to approximate that arriving at the boundary by taking variables $\vec{D}$ and $\vec{B}$ from the adjacent cell. By combining (1) and the physics that there is no penetration of magnetic field into the cylinder, i.e.,

$$\hat{n} \cdot \vec{B} = 0 \tag{2}$$

one can obtain a pair of the magnetic fields on the cylinder's peripheral surface. Recall that the total electric field intensity on the perfect conductor surface always vanishes if the conductor is stationary. For a circular cylinder made of perfect conductor rotating about its axis, every point on the surface has the instantaneous velocity and the normal vector being always perpendicular to each other. Consequently, there is no need to consider the relativistic effects even its angular velocity is greater than the light speed. It is therefore concluded that the tangential component of the electric field (z-directed) must vanish on the surface of a rotating circular cylinder. In the present simulation, the so called non-reflector slice of cylinder is defined such that on its surface the electric is zero in magnitude, and magnetic fields obey (2). Finally, on the most outer cell boundary, the boundary conditions ensure that there is no reflection of EM fields from this artificial wall.

4. NUMERICAL RESULTS

Since the application of the boundary conditions is independent of whether a perfect cylinder rotates, the scattered EM fields from both cases exhibit similar behaviors. Therefore, comparison of the scattered EM fields between from a stationary cylinder and from a rotating cylinder is omitted. The only difference is then the application of the PCSBG's technique. To start, a series of diagrams was given in Figure 5 illustrating the scattered electric field distribution over the numerical domain. The cylinder is solid, made of perfect conductor, and stationary at the center under the illumination of a Gaussian EM pulse. Diagrams 5(a) through 5(d) give the interaction between the cylinder and the EM pulse, as well the evolution of the electric fields. There are three parts: the scattered electric fields (dark open ring,
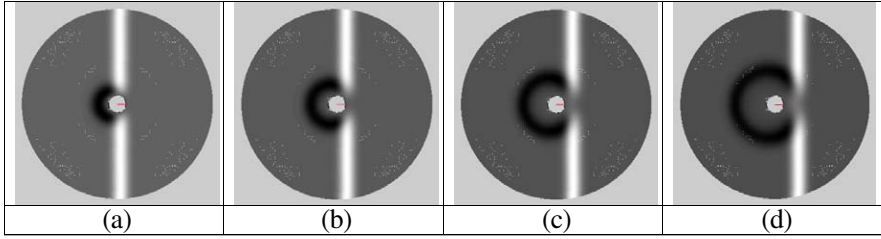
Figure 5. Electric field distributions: The cylinder as a whole is at rest. (Background: Zero, bright: Positive, dark: Negative).
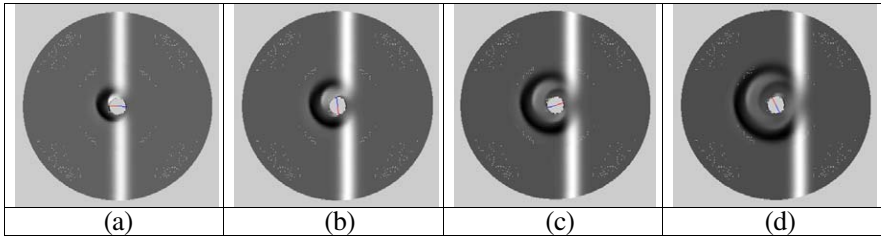

Figure 6. Electric field distributions: Two slices rotate two cycles. (Background: Zero, bright: Positive, dark: Negative).

negative in strength), the incident electric fields (bright bands outside the ring, positive in strength), and those behind the cylinder (blur). It is noticed that the incident EM pulse, though interacts with the cylinder, propagates straight in the positive x-direction despite the fact that the O-type grids are concentric. This is a consequence of that MOC takes all metric terms of each cell into consideration when it solves for the filed quantities.

A sequence of plots bearing the evidence that the cylinder is rotating and scattering EM fields all at once was given in Figure 6 where the cylinder has two halves and rotates two turns within the pulse duration. Note that the dark ring as in previous figure is mixed with bright haze curve lines and that there are a thin blur bright edge in front of and a broadened bright band behind the dark band. It is the evidence that the EM fields are scattered by the non-reflector slice of cylinder. Another sequence of plots was demonstrated in Figure 7 where the cylinder has four quarters and rotates one half turns. From these two sets of plots, it is observed that the scattered fields from the cylinder rotating at slower speed have blurry structure.

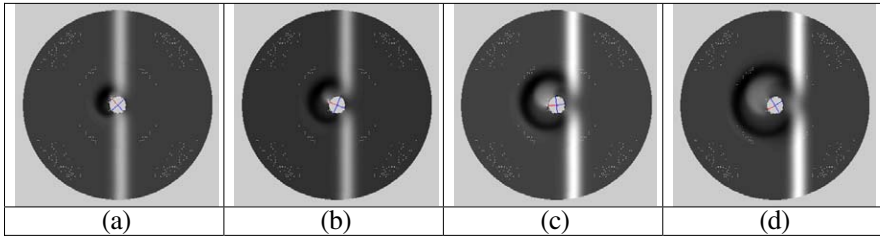For closer comparison on the effects of different velocities on

Figure 7. Electric field distributions: Four slices rotate one half cycles. (Background: Zero, bright: Positive, dark: Negative).
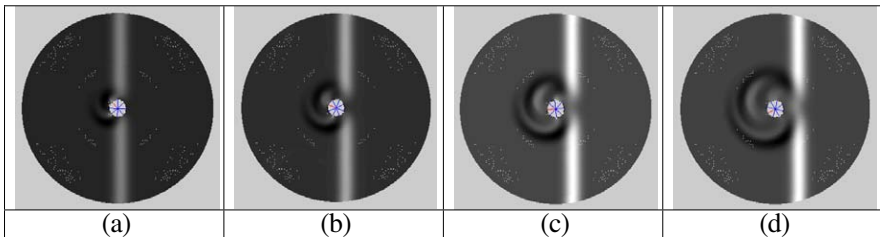

Figure 8. Electric field distributions: Eight slices rotate one half cycles. (Background: Zero, bright: Positive, dark: Negative).
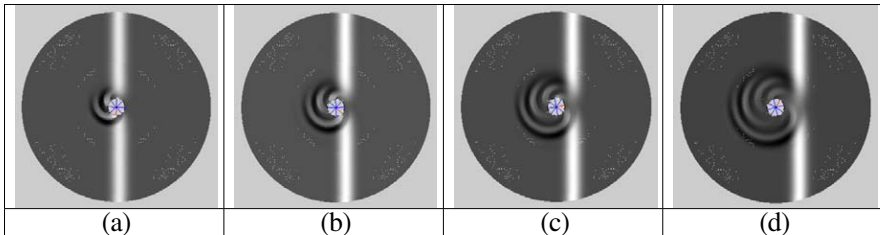

Figure 9. Electric field distributions: Eight slices rotate one cycle. (Background: Zero, bright: Positive, dark: Negative).

the scattered fields more simulations were carried out and given in Figures 8 through 10. The rotating cylinder is divided into eight slices alternating reflector with non-reflector and makes one half turns, one turn, and two turns, respectively. Similar phenomena were observed. Especially, the scattered EM fields form clear vortex structures for all these three cases. The scattered electric fields have sharper yet slenderer fringes between the positives and negatives when they are scattered from a cylinder rotating at faster velocities. It was shown
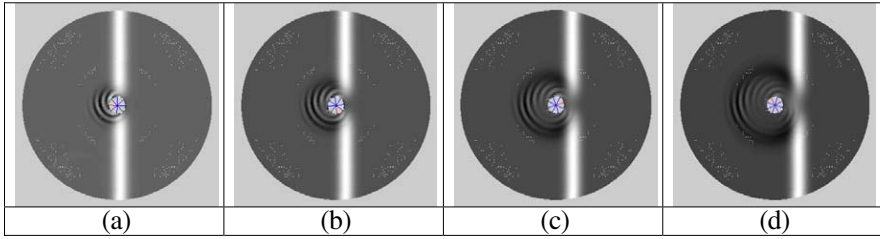
Figure 10. Electric field distributions: Eight slices rotate two cycles. (Background: Zero, bright: Positive, dark: Negative).

that the number of bend lines increases, and that the line becomes thinner as the cylinder rotates faster and faster. From all patterns, a contour of dark ring as in Figure 5 can always be identified though interfered by thin whirlpool-like bright lines.

5. CONCLUSION

The numerical results of the scattered electric fields from a rotating cylinder have been demonstrated in this paper. The computational results are obtained through the application of method of characteristics (MOC) combined with the passing center swing back grids (PCSBG) technique which has been clearly explained and evidently resolves the difficulty of grid distortion caused by rotating objects. The success of PCSBG is based on the nature of MOC that all field components are defined in the centroid of grid cell. Most field distribution patterns given in this paper have vortex structures as evidences of the fact that the cylinder is rotating and scattering EM fields simultaneously. It is planned to apply PCSBG/MOC to the prediction of the scattered EM fields by rotating objects of little complex yet symmetric structures where the relativistic effects can not be neglected.

REFERENCES

1. Holmes, J. F., "Scattering of plane electromagnetic waves by moving objects," *Proceedings of the IEEE*, Vol. 58, No. 5, 829–830, May 1970.
2. Cooper, J., "Scattering of electromagnetic fields by a moving boundary: The one-dimensional case," *IEEE Trans. Antennas Propagation*, Vol. 28, No. 6, 791–795, November 1980.

3. Harfoush, F., A. Taflove, and G. Kriegsmann, "A numerical technique for analyzing electromagnetic wave scattering from moving surfaces in one and two dimensions," *IEEE Trans. Antennas Propagation*, Vol. 37, 55–63, January 1989.

4. Cooper, J., "Longtime behavior and energy growth for electromagnetic waves reflected by a moving boundary," *IEEE Trans. Antennas Propagation*, Vol. 41, No. 10, 1365–1370, October 1993.

5. De Cupis P., P. Burghignoli, G. Gerosa, and M. Marziale, "Electromagnetic wave scattering by a perfectly conducting wedge in uniform translational motion," *Journal of Electromagnetic Waves and Applications*, Vol. 16, No. 8, 345–364, 2002.

6. De Cupis, P., G. Gerosa, and G. Schettini, "Electromagnetic scattering by an object in relativistic translational motion," *Journal of Electromagnetic Waves and Applications*, Vol. 14, No. 8, 1037–1062, 2000.

7. Ciarkowski, A., "Electromagetic pulse diffraction by a moving half-plane," *Progress In Electromagnetics Research*, PIER 64, 53–67, 2006.

8. Gaffour, L., "Analytical method for solving the one-dimensional wave equation with moving boundary," *Progress In Electromagnetics Research*, PIER 20, 63–73, 1998.

9. Gaffour, L., "Nature of electromagnetic field and energy behavior in a plane resonator with moving boundary," *Progress In Electromagnetics Research*, PIER 23, 265–276, 1999.

10. Censor, D., "Non-relativistic scattering in the presence of moving objects: The Mie problem for a moving sphere," *Progress In Electromagnetics Research*, PIER 46, 1–32, 2004.

11. Censor, D., "Free-space relativistic low-frequency scattering by moving objects," *Progress In Electromagnetics Research*, PIER 72, 195–214, 2007.

12. Borkar, S. R. and R. Yang, "Scattering of electromagnetic waves from rough oscillating surface using spectral Fourier method," *IEEE Trans. Antennas Propagation*, Vol. 21, No. 5, 734–736, September 1973.

13. Kleinman, R. E. and R. B. Mack, "Scattering by linearly vibrating objects," *IEEE Trans. Antennas Propagation*, Vol. 27, No. 3, 344–352, May 1979.

14. Van Bladel, J. and D. De Zutter, "Reflection from linearly vibrating objects: Plane mirror at normal incidence," *IEEE Trans. Antennas Propagation*, Vol. 29, No. 4, 629–37, July 1981.

15. Ho, M., "One-dimensional simulation of reflected EM pulses

from objects vibrating at different frequencies," *Progress In Electromagnetics Research*, PIER 53, 239–248, 2005.

16. Ho, M., "Scattering of EM waves by vibrating perfect surfaces simulation using relativistic boundary conditions," *Journal of Electromagnetic Waves and Applications*, Vol. 20, No. 4, 425–433, 2006.

17. Ho, M., "Scattering of EM waves from traveling and/or vibrating perfect surface: Numerical simulation," *IEEE Trans. Antennas Propagation*, Vol. 54, No. 1, 152–156, January 2006.

18. Ho, M., "Propagation of electromagnetic pulse onto a moving lossless dielectric half-space: One-dimensional simulation using characteristic-based method," *Journal of Electromagnetic Waves and Applications*, Vol. 19, No. 4, 469–478, 2005.

19. Van Bladel, J., "Relativistic theory of rotating disks," *Proceedings of the IEEE*, Vol. 61, No. 3, 260–268, March 1973.

20. Van Bladel, J., "Electromagnetic fields in the presence of rotating bodies," *Proceedings of the IEEE*, Vol. 64, No. 3, 301–318, March 1976.

21. Moaveni, M. K. and H. Vazifehdoost, "Rotating blades radio interference in a helicopter-borne CW doppler radar," *IEEE Transactions on Aerospace and Electronic Systems*, Vol. 17, No. 1, 72–82, 1981.

22. Zhang, Y., M. G. Amin, and V. Mancuso, "On the effects of rotating blades on DS/SS communication systems," *Proceedings of the Tenth IEEE Workshop on Statistical Signal and Array Processing*, 682–686, 2000.

23. Zhang, Y., A. Hoorfar, V. Mancuso, J. Nachamkin, and M. G. Amin, "Characteristics of the rotating blade channel for FH/FM communication systems," *Sixth International Symposium on Signal Processing and Its Applications*, Vol. 2, 493–496, 2001.